



EXPLORATIVE DATA ANALYSIS FROM MULTIPARAMETRIC MONITORING AT THE ACUTO FIELD LABORATORY (CENTRAL ITALY) FOR DETECTING PREPARATORY CONDITIONS TO ROCK BLOCK INSTABILITIES

GUGLIELMO GRECHI^(*), JENNYPER ROSA FERNANDES^(**), JEAN-PIERRE HU^(**),
ANNE-CHARLOTTE LE GALLAIS^(**), HUGO SAMPIERI^(**), GABRIELE AMATO^(*),
DANILO D'ANGIÒ^(***), MATTEO FIORUCCI^(****), ROBERTO IANNUCCI^(*),
GIAN MARCO MARMONI^(*) & SALVATORE MARTINO^(*)

^(*)Sapienza University of Rome - Earth Science department and CERI, Research Centre for Geological Risk - P.le Aldo Moro, 5 - 00185 Rome (Italy)

^(**)Polytech Sorbonne - Earth Sciences speciality - 4 Place Jussieu - 75005 Paris (France)

^(***)Department for the Geological Survey of Italy at the Italian Institute for Environmental Protection and Research (ISPRA) - Via Vitaliano Brancati, 48 - 00144 Rome (Italy). Formerly at the Department of Earth Sciences of Sapienza University of Rome and CERI Research Centre for Geological Risk

^(****)University of Cassino and Southern Lazio - Department of Civil and Mechanical Engineering - Via G. Di Biasio, 43 - 03043 Cassino (Frosinone, Italy)
Corresponding author: salvatore.martino@uniroma1.it

EXTENDED ABSTRACT

Il presente lavoro riporta i risultati preliminari delle attività di studio condotte presso l'Acuto Field Laboratory, laboratorio naturale del Dipartimento di Scienze della Terra (DST) presso Sapienza Università di Roma. Le attività hanno previsto l'analisi e il preprocessamento di serie temporali di dati acquisiti nel sito sperimentale, attività propedeutiche all'analisi esplorativa di relazioni cause-effettive tra forzanti ambientali e deformazioni indotte in ammassi rocciosi fratturati.

L'Acuto Field Lab, situato nell'ex cava Prenestina di Acuto (Frosinone), è stato progettato a partire dal 2015, nell'ambito di attività di ricerca condotte e sostenute dal Centro di Ricerca CERI per i Rischi Geologici, con l'installazione di sistemi di monitoraggio multi-parametrici e multi-sensoristici dedicati alla valutazione dell'influenza dei fattori preparatori ed innescenti l'instabilità d'ammasso dal breve al lungo termine. In questo primo periodo di vita, nel laboratorio naturale è stato monitorato un blocco di roccia, delle dimensioni di circa 20 m³, intensamente fratturato e predisposto ad evolvere per fenomeni di crollo. Il sistema di monitoraggio è composto da sensori per le condizioni meteorologiche, per la temperatura d'ammasso e di deformazione d'ammasso.

A partire dal 2018, le attività sperimentali condotte nell'Acuto Field Lab. sono finanziate nell'ambito dell'iniziativa "Dipartimenti di Eccellenza" supportato dal Ministero dell'Università e della Ricerca (MUR). In questo quadro, l'Acuto Field Lab è stato oggetto di un potenziamento strutturale, finalizzato ad indagare altri due nuovi settori della parete di cava e dell'implementazione di un nuovo sistema di monitoraggio integrato. In particolare, questi nuovi settori sono stati selezionati perché rappresentativi di diverse scale dimensionali e cinematismi di instabilità differenti, caratterizzati da diversi gradi di libertà. Il nuovo sistema di monitoraggio, operativo dall'inizio del 2022, ha integrato nuovi strumenti per il monitoraggio delle temperature d'ammasso, di flussi termici, delle condizioni idrauliche nei giunti, e delle deformazioni d'ammasso, anche grazie all'installazione di un innovativo sistema in fibra ottica differenziale, delle condizioni dinamiche e vibrazionali, grazie a micro-accelerometri, geofoni e sensori per le emissioni acustiche. Tutti i sensori installati sui tre differenti settori, acquisiscono i dati in continuo grazie a specifici *datalogger*. Inoltre, tramite un ponte radio, tutti i dati registrati vengono trasferiti via internet in tempo quasi reale presso l'infrastruttura server del DST essendo così fruibili per le successive analisi ed elaborazioni.

I risultati preliminari dell'analisi dati condotta, hanno posto in luce come il fattore preparatorio termico sia quello maggiormente agente sulla superficie dell'ammasso roccioso, il quale opera attraverso cicli deformativi termo-indotti sia alla scala diurna che alla scala stagionale. In questo studio sono riportate le prime risultanze per i nuovi settori strumentati della parete di cava, per oggetti a diversa scala dimensionale. Inoltre, per un intervallo temporale di circa un anno, particolare attenzione è stata posta all'azione preparatoria che può essere rappresentata dalla ventilazione o da raffiche di vento sugli effetti registrati a carico dell'ammasso roccioso fratturato, valutando la direzione di provenienza del vento rispetto all'esposizione della parete. Grazie alla compilazione di script dedicati, si è proceduto al calcolo delle deformazioni residue non recuperate nel ciclo elastico diurno, o alla valutazione di effetti di gelività dell'ammasso roccioso stante i parametri ambientali, quali la temperatura, il tasso di umidità e la presenza di precipitazioni avvenuti durante o nei giorni antecedenti quelli analizzati.

Il presente studio si prefigge lo scopo di presentare le risultanze preliminari ottenute dall'analisi delle serie temporali di monitoraggio ottenute per i settori di cava strumentati all'inizio del 2022. Queste saranno approfondite nel tempo e vedranno affiancarsi i primi risultati provenienti dai sistemi di monitoraggio tecnologicamente più avanzati, come quelli dell'*array* in fibra ottica basato su celle di Bragg (FBG *array*). Le occorrenze di deformazioni anelastiche, non recuperate durante cicli termici diurni e stagionali, verranno comparate con dati microsismici e acustici provenienti dall'ammasso, valutando l'evoluzione del numero e dell'energia dei segnali registrati in relazione all'ampiezza delle forzanti agenti nel sito, con l'obiettivo di valutare segnali vibrazionali sintomatici di deformazioni plastiche o precursori di effetti irreversibilità a carico di microfratture in grado di anticipare crolli e rotture in roccia.



ABSTRACT

This study summarises the research activity carried out in the Acuto Field Laboratory (FR, Italy), where experiments testing the stability of a subvertical rock wall in limestone are ongoing within an abandoned quarry, now devoted to studies focused on the mitigation of geological risks. The research focuses on the natural factors that can prepare a subvertical rock mass to evolve through subsequent rock fall if predisposing conditions are verified. A network of multiparameter monitoring sensors is installed on three different sectors of the rock wall to record both the natural and anthropogenic stressors and the effects of deformation induced by them. In terms of stressors, the multiparametric monitoring system is able to detect the environmental parameters, such as temperature, rainfall, wind, strain, and vibrations. In terms of induced effects on the rock mass, the multiparametric monitoring system is suitable to detect deformation, displacement, and microseismicity. In this paper, the different monitored parameters are presented along with detailed analyses to highlight cause to effect relationships, such as freezing and thawing, to retrieve correlations among different factors. The obtained results represent the first analysis of the data recorded in the three instrumented sectors of the field laboratory and allowed evaluating the role of preparatory factors in inducing rock falls, opening further perspective on numerical modelling or machine learning applications based on monitoring data.

KEYWORDS: *Multiparameter monitoring, rock fall, environmental forcings, preparatory factors, data analysis*

INTRODUCTION

The effect of near surface temperature fluctuations is considered in literature one of the less-immediate causes of slope instability, since their daily actions are featured by low intensity and are limited in depth within the shallowest layers of slopes (GUNZBURGER *et alii*, 2005). Despite this, seasonal temperature variations can extend their influence at greater depth involving greater volumes of rock masses, cumulatively operating a mechanical preparation for external triggers (MARMONI *et alii*, 2020), which can be natural or anthropogenic (FINNEGAN *et alii*, 2022). This periodic and continuous stress is also able to drive the evolution of rock blocks up to the ultimate failure as a fatigue process, causing irreversible damaging, concentrating stresses, and leading to a slow progressive failure (GASC-BARBIER *et alii*, 2019; GISCHIG *et alii*, 2011a, b).

The understanding of how and when such irreversible effects can take place after completing daily or annual cycles is one the most challenging frontier in engineering geology (TABOADA *et alii*, 2017), since from this prediction, the most suitable countermeasures and mitigation strategies could be implemented (FIORUCCI *et alii*, 2020). These interventions

become challenging when dealing with rock fall and rock block instabilities that can rapidly evolve without evidence of antecedent deformations. In this sense, the evaluation of precursor signals based on remotely sensed or geophysical data (i.e., the counting of microseismic and acoustic signals or frequency shifts in the eigenmodes of geometrically defined blocks) are crucial for a customised rockfall hazard assessment (BOTTELIN *et alii*, 2013; GEIMER *et alii*, 2022; GUILLEMOT *et alii*, 2022). The detection of permanent changes in physical and mechanical parameters of rock masses represents an important target to mitigate the related landslide risk as it can lead to catastrophic failures, especially when infrastructures are involved.

The study here presented is focused on the evaluation of the impact of environmental conditions and vibrations on the rock mass deformation, analysing data recorded by a multiparametric monitoring system installed in an abandoned quarry in the Municipality of Acuto (Frosinone, Italy), where the Acuto Field Laboratory (hereafter Acuto Field Lab), managed by Sapienza University of Rome and CERI Research Centre for Geological Risks, has been designed and implemented since 2015 for the analysis of environmental forcings on jointed rock mass. At this test site, a multi-parametric monitoring system including environmental, geotechnical, geophysical, and remote sensing devices, is devoted to evaluating the influence of external stressors on the short- to long-term stability of an intensely jointed rock wall and to detecting precursors of rock failure by means of acoustic and microseismic devices.

In the last years, several field experiments and test-site have been implemented worldwide (BAKUN-MATZOR *et alii*, 2013; COLLINS *et alii*, 2018, 2019) with the goal of understanding thermally induced failure mechanisms and of how periodic stressors are able to lead rock masses to failure also in the absence of evident triggering factors. The Acuto Field Lab fits into this framework, and both contact and remote monitoring devices are deployed in site to record these different environmental and vibrational events that could drive rock mass deformations.

For this purpose, we must consider three categories of factors that affect the slope stability:

- predisposing factors: that are inherited by the rock mass throughout its geological history, can be considered static in the time window of evolution of the considered process. In this group can be listed the lithology, joint attitude and surface conditions, slope angle and rock mass geometry;
- preparatory factors: which are those low intensity stresses that take place cyclically and continuously in a medium- long-time window and whose cumulative action over time moves the system from equilibrium to conditions close to failure;
- triggering factors: consisting in short-term and high

magnitude forcings, such as earthquakes, intense rainfalls or windstorms, which can lead the slope toward failure conditions.

The importance of studying the possible natural factors leading to rock mass failure or surface exfoliation (e.g., in granitoid or metamorphic rocks) become more important in natural heritage contexts, where active geotechnical consolidations or invasive structural interventions become impossible. In a climate change perspective, the reliability of this study is strongly dependent on the time duration and data completeness derived from the monitoring system, which must be long enough to collect trend changes or non-ordinary events capable of inducing plastic deformations.

From the broad type of sensors, the collected sets of information can become suitable for the long-term analysis of the rock mass behaviour, whose physical and mechanical properties can be a proxy of growing instabilities. Such analysis is far from being deterministic in nature, therefore it has to be managed considering machine learning or artificial neural network approaches that require massive datasets.

Herein, a preliminary overview of the field laboratory and of the available dataset is provided, showing the dataset preparation and preprocessing activities carried out in observation- or statistically based approaches. The different tasks and processed data are then discussed, showing the preliminary obtained results about the time-series analysis carried out and the comparison among the studied sectors of the rock mass hereafter performed. First insights and future advances in the Acuto Field Lab are also discussed.

THE ACUTO FIELD LABORATORY

The Acuto Field Lab is a natural laboratory characterised by a subvertical quarry rock wall 500 m long and 50 m high, composed of Cretaceous limestones that are intensely fractured by the subsequent stages that featured the formation of the Apennine orogen and the opening of the Tirrenian back-arc basin. The limestones are micritic, wackestone according to Dunham classification, and are dissected by several joint sets, locally conjugated and geostructurally oriented with respect to the direct and transtensive faulting systems locally visible along the quarry face (Fig. 1).

The natural laboratory is in the municipality of Acuto (FR, Italy), a small municipality located southeast of Rome with about 1800 inhabitants. The quarry, originally devoted to the excavation of inert rockfill, remained active till the end of '70 (Fig. 2). To date the manual excavation activities, supported by controlled explosion, carved the carbonatic hill (Fig. 2) creating a vertical cliff that is highly predisposed to experience detachment of rock blocks with size up to some cubic metres (Fig. 1).

Nowadays this limestone quarry is not exploited anymore and was abandoned without implementing any recovery operations. Given the high risk related to rock landslides, its access is now forbidden to inhabitants. As an indirect measure to recover the use of this area, the local municipality conferred the loan to Sapienza University of Rome, for carrying on research, didactic and dissemination activities related to geological risks, thus representing an exemplary recovered site without the implementations of invasive structural interventions or remediations.

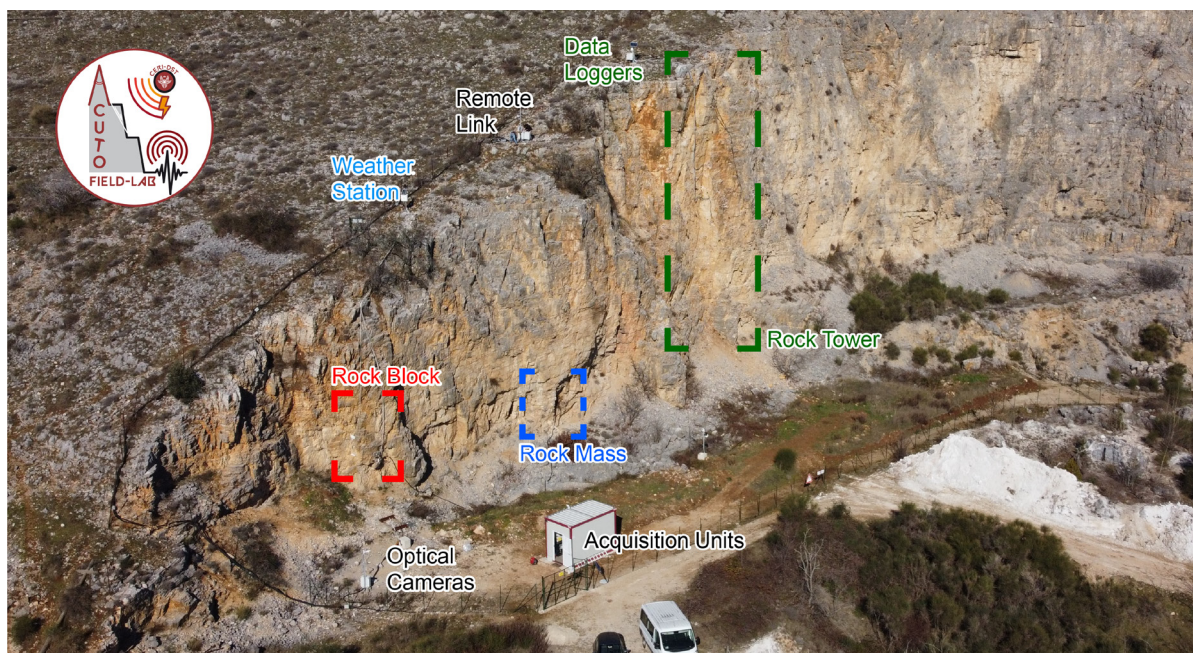


Fig. 1 - Panoramic view of the instrumented sectors in the Acuto Field Laboratory inside the abandoned quarry (Frosinone, Central Italy)

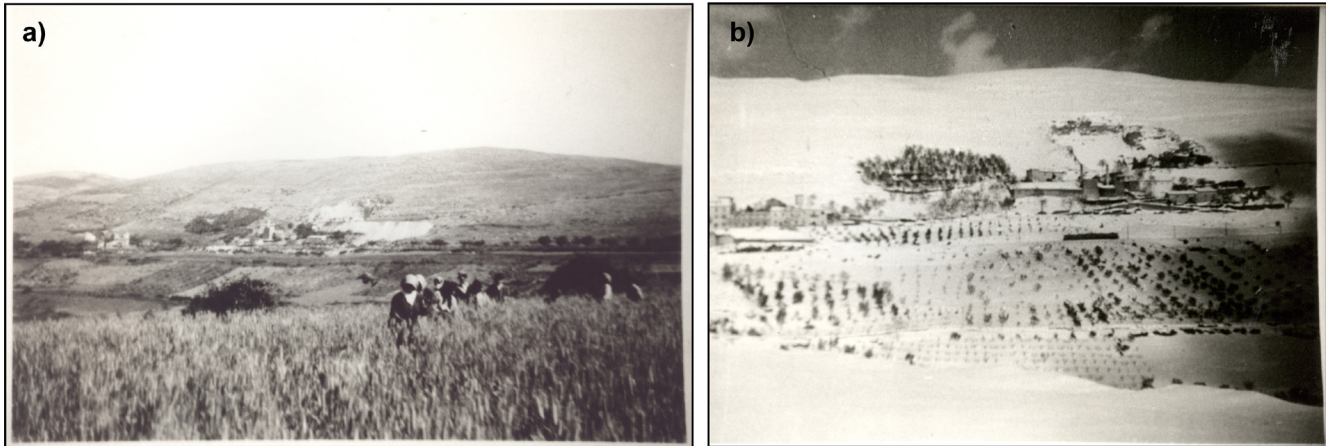


Fig. 2 - View of the Acuto quarry excavation during the 50's. Photographic Archive of Acuto community. Photo Credits to Associazione Culturale "L'occhio e la memoria"

In the Acuto Field Lab, three different sectors were identified and monitored: i) a rock block sector, where a 20 m³ rock block is jugged and prone to evolve by a rock fall mechanism; ii) a rock tower isolated from the rock wall behind by vertical open joint and free to move and evolve by rock toppling mechanism (HUNGR *et alii*, 2014); iii) a stable rock mass sector where no evidence of protruded blocks can be found.

In this study, we focused on the two experimental rock wall sectors characterised by well-defined kinematics and distinguished dimensional scale of the involved blocks.

As reported in Fig. 3, these two monitoring sectors are characterised by well-defined and sharp geometries that highlight two main surfaces (i.e., front, and back with respect to the rock wall overall direction), which are in turn marked by a different exposure to the incident solar radiation. In each of these sectors, the different groups of sensors were distinguished and compared to perform a detailed data analysis and to account for different behaviours related to solar radiation (FIORUCCI *et alii*, 2018). The collected data allowed us to evaluate the long-term behaviour of the rock mass (i.e., rock matrix and joints) exposed to environmental forcings and to assess their role in the generation or propagation of cracks.

Environmental data have been continuously monitored since 2015 with a 1-minute time sampling over the top and bottom of the quarry, monitoring air temperature and humidity, total rainfalls, wind speed and direction.

From the meteo-climatic point of view, thermo-pluviometric data recorded from 2000 to 2015 by the closest weather station - located 5 km far from the Acuto Field Lab - revealed a monthly average air temperature showing its maximum during Summer, with average maximum temperatures that reach over 30 °C in July-August, while the coldest months are January and February with average minimum temperatures around 1.5

°C. The monthly average rainfall shows a peak in Autumn, with values in the order of 120-130 mm/month. The minimum rainfall is clustered in Summer (38 mm/month), coinciding with the maximum thermal peak. These weather features allow the attribution of this area to the temperate Mediterranean climatic region.

Both the above-mentioned sectors of the site (i.e., Tower and Block) had several devices installed for different purposes. The rock block is instrumented with thermal and strain devices, including: two rock thermometers (TS), one heat flux cell (HFC), one leaf wetness sensor (LWS), six strain-gauges (SG) on rock matrix and microfractures and three joint-gauges (F) on open fractures. In addition, geophysical sensors were also installed: a three-component 10 Hz and one three-component 4.5 Hz geophone, four Acoustic Emission (AE) sensors with 150 kHz nominal frequency. The rock tower, recently instrumented thanks to the financial support granted in the frame of the Department of Excellence 2018-2022 initiative, is instrumented with two thermal profile probes (Tf and Tb, composed by four thermocouples installed at progressively greater depths from 10 to 40 cm), one leaf wetness sensor, six strain-gauges, three joint-gauges, six three-component 10 Hz geophones, two three-component 4.5 Hz geophones (Fig. 3). In addition to the instrumentation installed on the two sectors, other sensors were deployed in the stable rock mass portion, in particular: two three-component 4.5 Hz geophones and two three-component 10 Hz geophones installed one pair at the top and one pair at the base of the slope. All the geophones were cable-connected to a total of seven digital data loggers (VMR), set with a sampling frequency of 1000 Hz for the 10 Hz geophones and of 500 Hz for the 4.5 Hz geophones. Besides, two three-component force balance accelerometers (EpiSensor) cable-connected to a Kinematics Quanterra Q330 digital data-

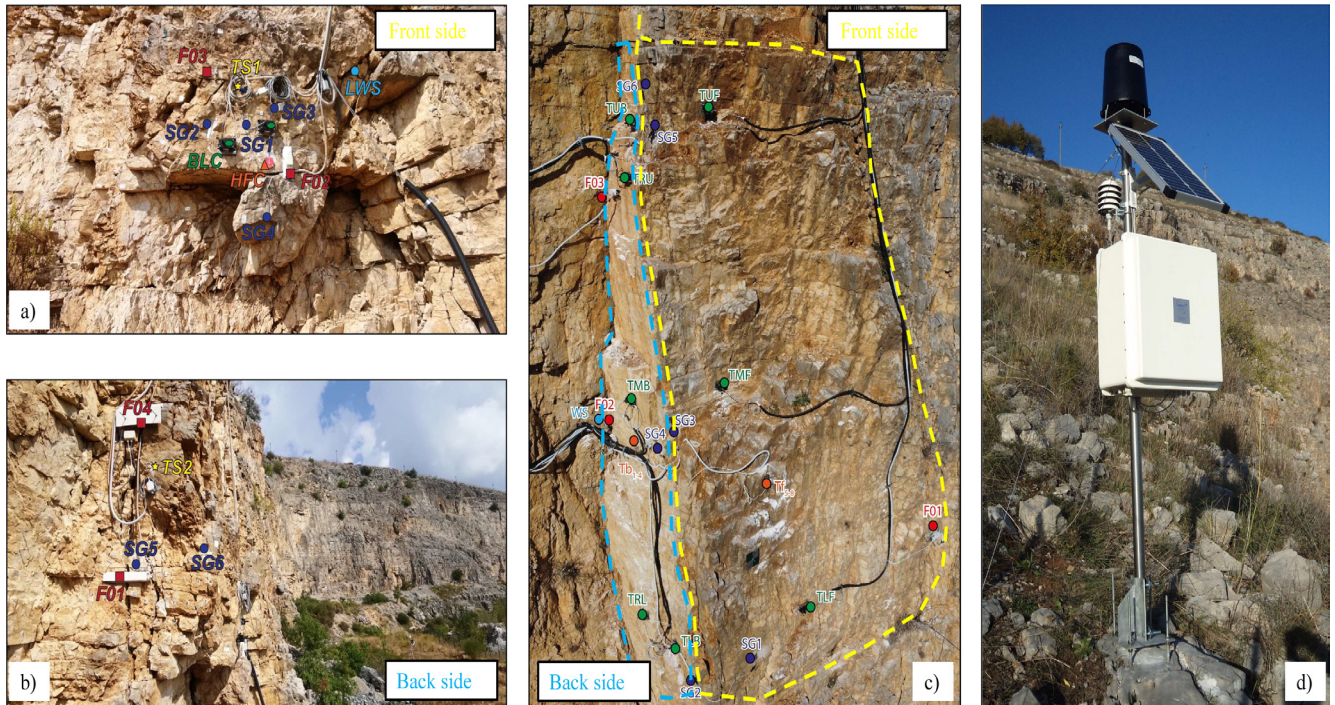


Fig. 3 - Photographs of the different sectors with the installed instruments at the Acuto Field Lab: a) Front face of the Block sector; b) Back face of the Block sector; c) the Tower sector with its front and back faces; d) weather station with box containing Campbell Scientific data logger of rock strain, displacement, and thermal sensors

logger and one fibre Bragg grating array implemented with three baselines and nine measurement points are deployed in the Rock Mass Sector (Fig. 1). The monitoring system is connected to specific digital datalogger, which allow for continuous and triggered acquisition modes. The power supply is guaranteed by the local low-voltage electrical infrastructure, solar panels, and multiple backup batteries. Besides, internet services for real-time transfer of all recorded data to a cloud storage server, located inside the Department of Earth Sciences of Sapienza University, are guaranteed by a radio link.

Together with the on-site monitoring, remote acquisitions were also carried out at the Acuto Field Lab with laser scanners and drones for the reconstruction of the 3D volumetry of the monitored sectors (FANTINI *et alii*, 2017) and with a thermal imaging camera for the study of the thermal behaviour of the rock mass on 2D surfaces (FIORUCCI *et alii*, 2018) and on specific 3D volumes (GRECHI *et alii*, 2020).

PROCESSED DATA

The above-described multiparametric monitoring system, allowed to obtain data about deformation, vibrations, weather, and rock temperature, also by means of remotely sensed data (i.e., IR thermography). The analysis focused on a temporal coverage starting from January 2021 to July 2022. Data processing was managed by the open-source web application Jupyter notebook.

In this work, we preliminary analysed environmental and strain data recorded at both the rock tower and the rock block. The different thermocouples (TS) installed for measuring temperature at different depths were named with a number representing their position. TS1 and TS2, located on the Block sector, are both at a depth of 8 cm with the first one installed on the front face and the second one on the back face. The front face, exposed to the East, is hit by solar radiation as soon as the sun rises, while the back face, exposed to the south, receives the solar radiation later in the afternoon, with a peak of temperature delayed after 14:00. On the Tower sector, thermocouples TS1 to TS4 are located on the front face with depths of 33, 23, 13 and 3 cm, respectively; same depths at which thermocouples TS5 to TS8 are installed on the back face. About the strain gauges (SG) of the Block sector, SG1 to SG4 are installed on the front along with extensometers F2 and F3, while SG5 to SG6 are placed on the back face along with extensometers F1 and F4. At the Tower sector SG1, SG3, SG5 and extensometer F1 are on the front face; lastly, SG2, SG4, SG6 and extensometers F2, F3 are on the back face (Fig. 3). The dataset obtained by the strain gauges span from January 2021 to April 2022 for the Block sector and from January to July 2022 for the Tower sector that was the last being instrumented.

Temperature distribution over the rock tower sector was additionally evaluated by means of remote sensing approach,

trying to derive daily thermal cycles and comparing it with the ones extracted at the most surficial level by contact monitoring (i.e., rock thermocouples). Remotely InfraRed Thermography acquisitions were thus approached in specific days by using a FLIR T-840 thermal camera mounted on a tripod. The contribution of solar radiation on protruded rock block was inferred, highlighting the presence of the thermally resistive open joint behind the rock tower.

Wind data are recorded as m/s for the speed and in terms of azimuth for the direction. Temporal coverage of the wind data was also evaluated, checking for irregularities or lack of data in the analysed period. Afterwards, specific windy events were analysed, focusing on intensity and directional distribution with respect to the rock blocks orientation. Windy days were classified according to the Beaufort scale, an empirical measure that relates wind speed to observed conditions at sea or on land.

In the considered time windows, vibrational data collected from the geophones were also processed with the aim of i) define an automated procedure to perform common pre-processing operations as trend and mean removal to obtain one-hour long time histories; ii) check of the earthquakes occurred in the surroundings of Acuto within the recorded time histories; iii) approaching an inventory of microseismic signals.

PRELIMINARY RESULTS

Wind Analysis

The purpose of the wind analysis was to analyse the different behaviours of the wind and to correlate them with the strain and geophones data. Raw data showed erroneous readings between January and July 2021 (Fig. 4) due to malfunctions of the anemometer, therefore, we will not consider them for the analyses discussed here.

In our study, we compared the orientation of the rock Tower and of the rock Block with the wind direction to point out if wind was hitting the different faces of the block and the tower.

The front face of the rock tower and of the rock block are

exposed to the North at about 10°. The back face of the Block and the Tower have different orientations: the one of the Block is exposed to the South while that of the Tower is exposed rather to the East. We will discuss later that these two different orientations influence the temperature.

Over the period starting from January to July 2022, no storms were detected; the wind speed never exceeded 70 km/h (Fig. 5), however large interruptions can be observed in the time series. Based on the Beaufort scale (Tab. 1), we classified the wind into two main categories, the 'Breeze' and the 'Gale', that can cause small effects on land. A wind speed between 30 and 50 km/h corresponds to a 'Breeze' and a wind speed between 50 and 70 km/h corresponds to a 'Gale'.

In Fig. 6a, red points correspond to wind speeds varying from 50 to 70 km/h. We can see that only one period corresponds to a 'Gale', in April 2022, more precisely on the 21st around 9 a.m.

All Gales from January to July 2022 (Fig. 7) are oriented towards the East, i.e., 90° from the front of the Tower and the Block, and from the back part of the Tower.

The colour scale indicates the wind speed, while the size of the sections represents the frequency at which this wind occurs. Lighter winds, the 'Breeze', are much more frequent (Fig. 8) and we still see an average direction towards the East or Northeast (Fig. 9).

Analysing all the wind roses on the 'Breeze' type over the whole period, the average wind is oriented towards the East which corresponds to the back part of the tower but also with a more or less 90° orientation on the front part of the Tower and the Block.

However, there are different behaviours when the wind direction is towards the South or the West (Fig. 10). These behaviours correspond only to wind speed between 30 and 50 km/h. For this behaviour on July 8, 2022, we could see a link with the temperature on the same date.

Rainfall Analysis

In Fig. 11, it is shown the cumulative rainfall over the last

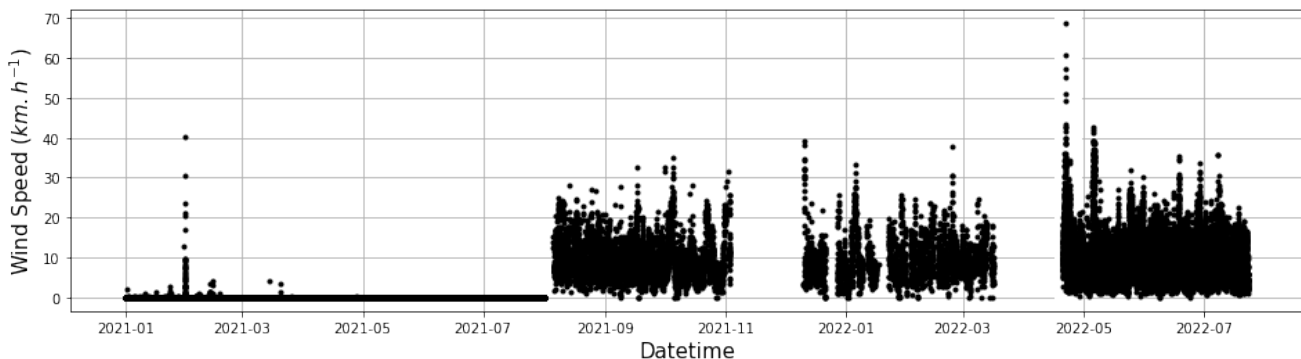


Fig. 4 - Wind speed from January 2021 to July 2022. The lack of data indicates a period of non-acquisition by the anemometer or its malfunctions (period with data constantly at zero)

EXPLORATIVE DATA ANALYSIS FROM MULTIPARAMETRIC MONITORING AT THE ACUTO FIELD LABORATORY (CENTRAL ITALY) FOR DETECTING PREPARATORY CONDITIONS TO ROCK BLOCK INSTABILITIES

Beaufort number	Wind Speed (mph)	Seaman's term		Effects on Land
0	Under 1	Calm		Calm; smoke rises vertically.
1	1-3	Light Air		Smoke drift indicates wind direction; vanes do not move.
2	4-7	Light Breeze		Wind felt on face; leaves rustle; vanes begin to move.
3	8-12	Gentle Breeze		Leaves, small bells in constant motion; light flags extended.
4	13-18	Moderate Breeze		Dust, leaves and loose paper raised up; small branches move.
5	19-24	Fresh Breeze		Small trees begin to sway.
6	25-31	Strong Breeze		Large branches of trees in motion; whistling heard in wires.
7	32-38	Moderate Gale		Whole trees in motion; resistance felt in walking against the wind.
8	39-46	Fresh Gale		Twigs and small branches broken off trees.
9	47-54	Strong Gale		Slight structural damage occurs; slate blown from roofs.
10	55-63	Whole Gale		Seldom experienced on land; trees broken; structural damage occurs.
11	64-72	Storm		Very rarely experienced on land; usually with widespread damage.
12	73 or higher	Hurricane Force		Violence and destruction.

19-31 mph = 30-50 km/h → Breeze
 32-46 mph = 51-74 km/h → Gale

Tab. 1 - Beaufort scale, images taken by <https://www.ikointl.com/it>

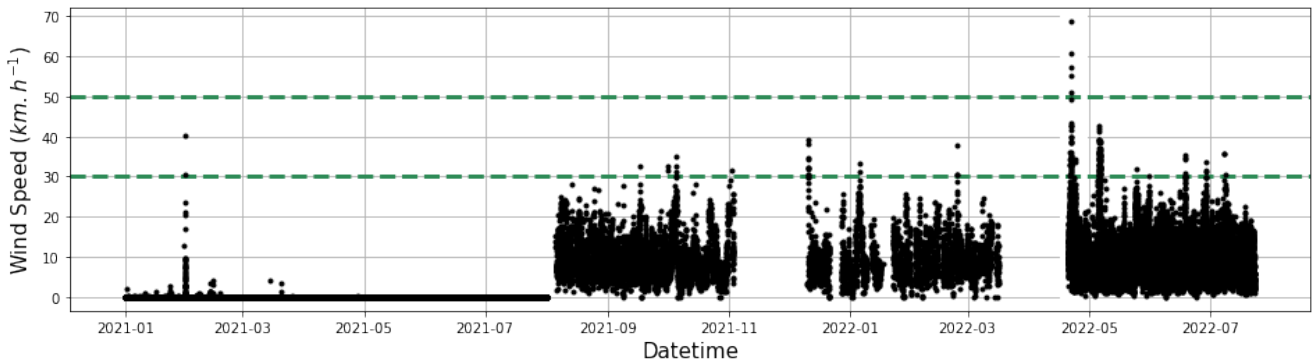


Fig. 5 - Wind speed from January 2021 to July 2022. The two dashed green lines represent the limit of the "Breeze", included between them

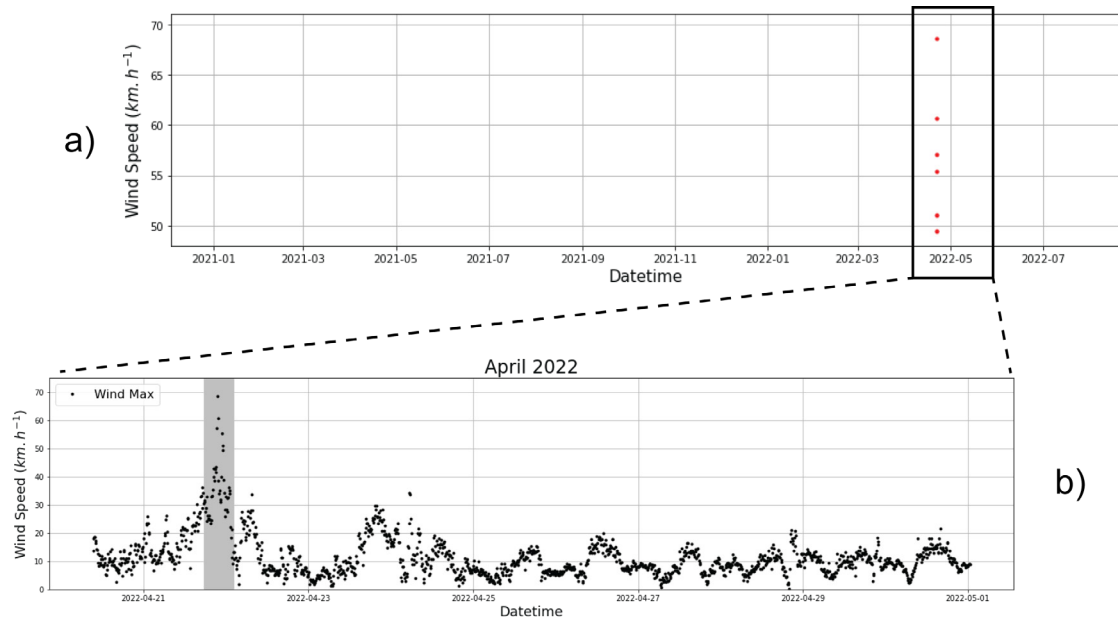


Fig. 6 - Graphs representing winds exceeding 50 km/h: a) Gale over the period from January 2021 to July 2022; b) Gale of April 2022. The grey boxes or areas represent 'zooms' on certain periods

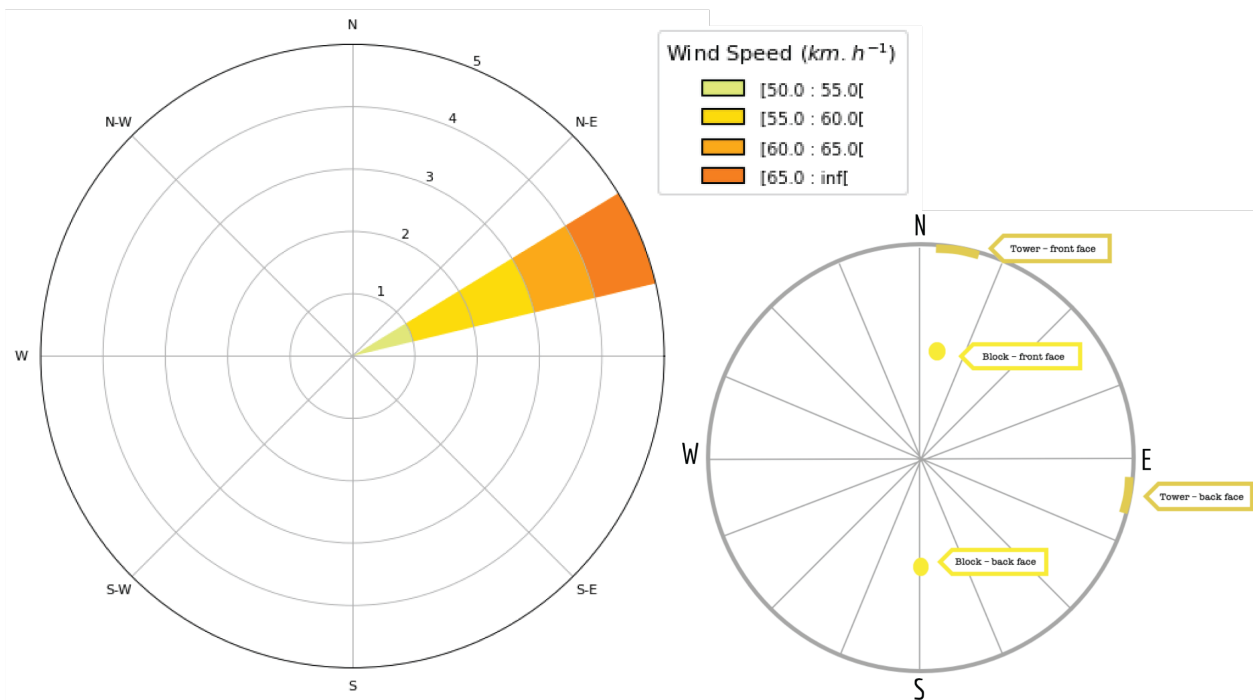


Fig. 7 - Rose diagram showing: on the left, the 'Gale' recorded on April 21st, 2022, at 9:00 p.m.; on the right, the orientations of the two study areas BLOCK (yellow) and TOWER (green) in their front and back faces

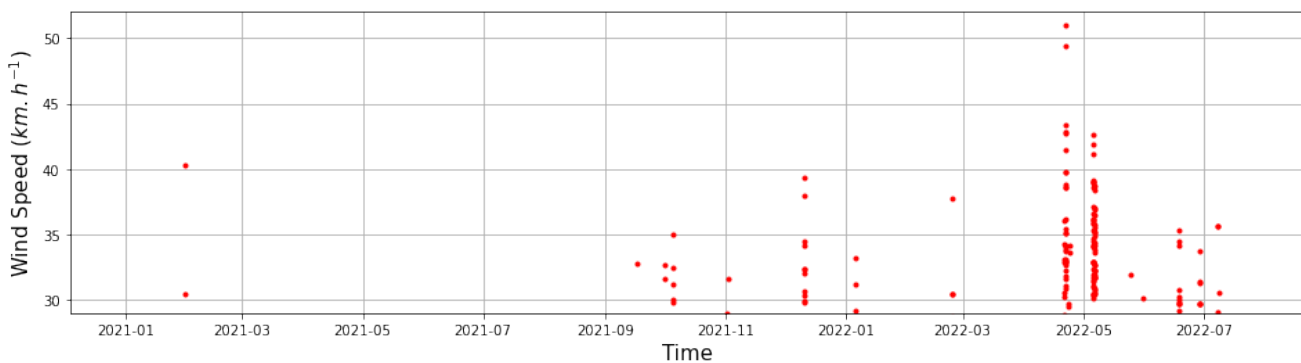


Fig. 8 - Graphs representing winds between 30 and 50 km/h from January 2021 to July 2022

two years. The black bars correspond to the rainfall measured in one day. However, despite the analysis over the entire 2021-2022 period, there is little, or no rainfall recorded from August 2021. Therefore, we believe that the pluviometer experienced some data recording issues from that date on. During rainfall, rain seeps into the rock joints and can freeze during the winter months. The rainfall data could be correlated with the other variables.

Temperature variation in rock mass

For a more detailed analysis of temperature variation, the results are here discussed first for the rock Block sector, and following for the rock Tower; finally, the results are compared

with each other. By analysing the data of the rock Block, we can see that both temperature sensors (i.e., front and back side thermocouples) show the same behaviour, i.e., they increase and decrease at the same rate, as demonstrated in the next Figure (Fig. 12). It is important to say that the sensor at the back of the rock Block was installed later than the installation of the first one, so between January and August 2021, only the data obtained by TS1 are represented. The fact that the back side of the rock Block has higher values is not surprising, as it is southward facing and exposed to the solar path approximately till 15:00. This agrees with the thermographic observations reported by FIORUCCI *et alii* (2018) for this site. Thermocouples installed in the rock block

EXPLORATIVE DATA ANALYSIS FROM MULTIPARAMETRIC MONITORING AT THE ACUTO FIELD LABORATORY (CENTRAL ITALY) FOR DETECTING PREPARATORY CONDITIONS TO ROCK BLOCK INSTABILITIES

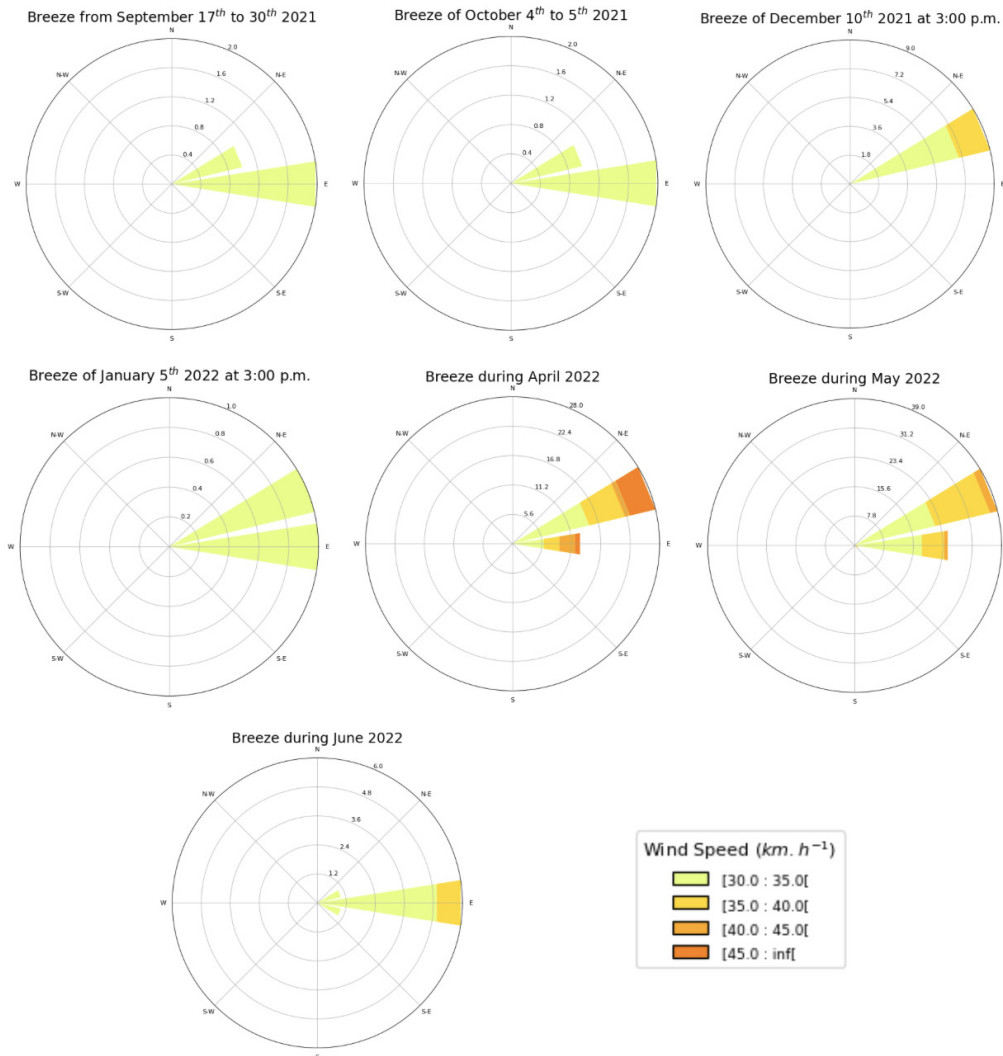


Fig. 9 - Wind rosette plots for the ‘Breeze’ recorded between January 2021 and July 2022. The colour scale indicates the wind speed. The size of the sections represents the frequency at which this wind occurs.

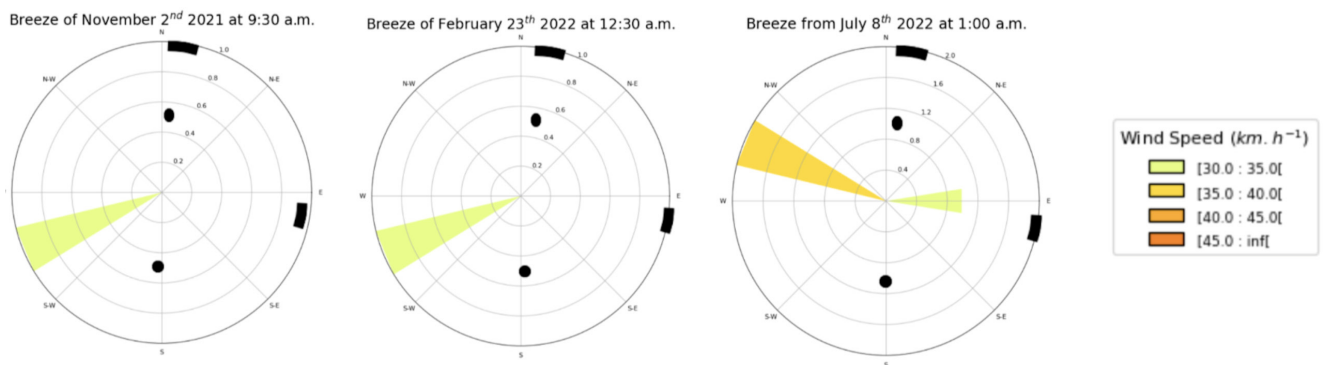


Fig. 10 - Anomalous behaviour in the direction of the ‘Breeze’ type wind. The colour scale indicates the wind speed. The size of the sections represents the frequency with which this wind occurs. The black icons represent the orientations of the studied areas, the rock Tower and the rock Block (see Fig. 4). The black icons represent the orientations of the studied areas, the rock Tower and the rock Block (see Fig. 4).

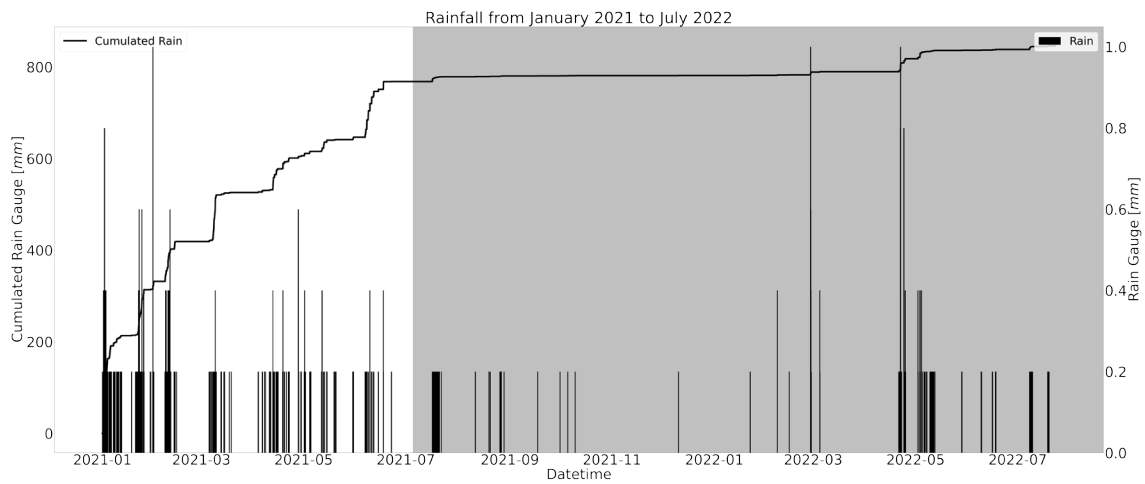


Fig. 11 - Rainfall recorded between January 2021 and July 2022. The curve represents the cumulative rainfall over the entire period. The bars represent the rainfall recorded on a single day

are representative of the behaviour of the rock matrix, since in the very first level (first centimetres) no fractures or open joints can be found.

During the period when TS2 was not yet installed, it is possible to compare the temperature inside the rock (8 cm from the surface of the front face) with the air temperature of the site (Fig. 13). The temperature inside the rock is slightly higher than the local air temperature, due to the heat absorption capacity of the rock exposed to solar irradiation.

Regarding the sensors located in the rock Tower, analogous trend can be derived, however the highest temperature is registered in the front face of the rock mass. From a comparison between sensors that are in the same position, but at different depths from the surface (3 and 33 cm depth: Fig. 14 and Fig. 15 respectively). Issues in the recorded time series were also found and attributed to error in the polynomial conversion of voltage

data in engineering units, that limited the minimum temperature reached by the series. The adopted pre-processing procedure allows to fix the bug and collect accurate temperatures.

In summary, the sensor closest to the rock surface records the highest and lowest temperature values, i.e., a greater variation than the one furthest from the surface, which is to be expected as the one furthest from the surface does not capture as much. This is consistent with the expected and in agreement with the heat conduction law (CARSLAW & JAEGER, 1959). Sensible variation of temperatures can be appreciated since the thermocouples fall within the daily thermal active layer (TAL).

Based on the above reported analysis it is possible to state that the back face of the rock Block has higher temperature values than its front face, while an opposite behaviour can be observed for the rock Tower; this resulting evidence is explained with the different elevation of the sensor from the ground and an angular incidence

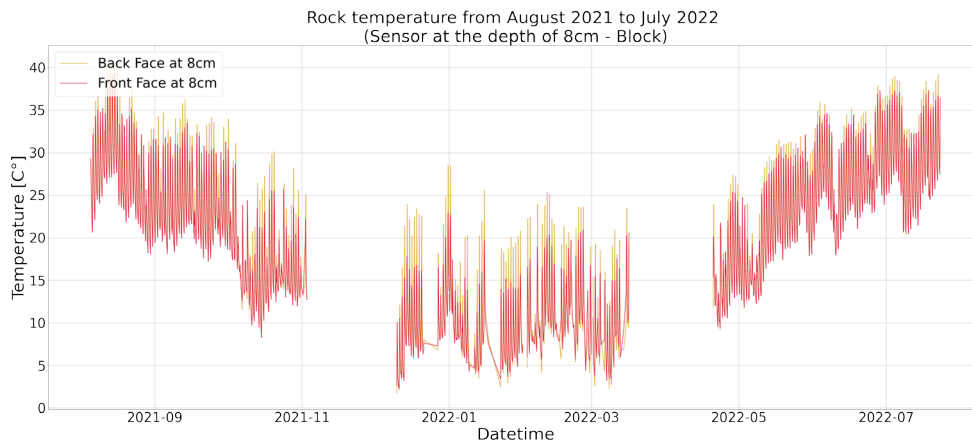


Fig. 12 - Rock temperature time-series in the rock Block for both front and back side, recorded at 8 cm depth

EXPLORATIVE DATA ANALYSIS FROM MULTIPARAMETRIC MONITORING AT THE ACUTO FIELD LABORATORY (CENTRAL ITALY) FOR DETECTING PREPARATORY CONDITIONS TO ROCK BLOCK INSTABILITIES

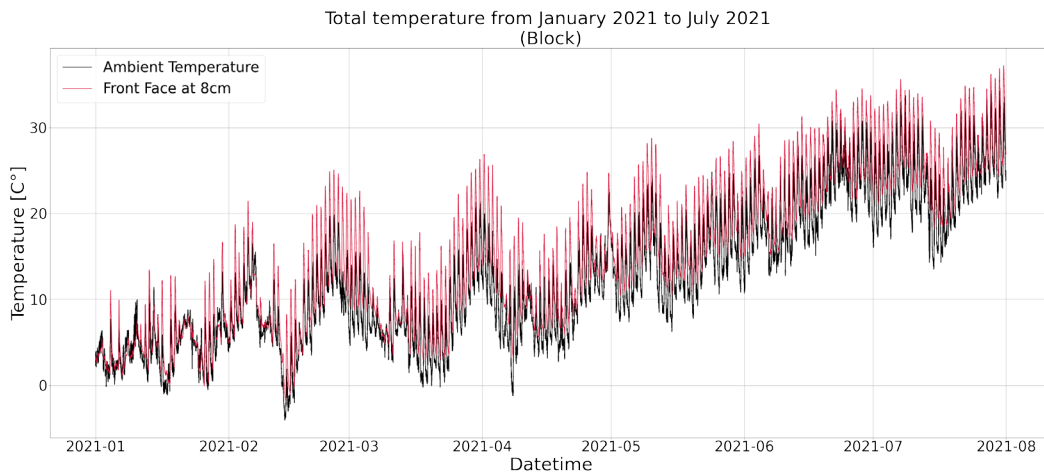


Fig. 13 - Air temperature recorded by the weather station at the top of the slope and rock temperature recorded 8 cm depth in the front face of the rock Block

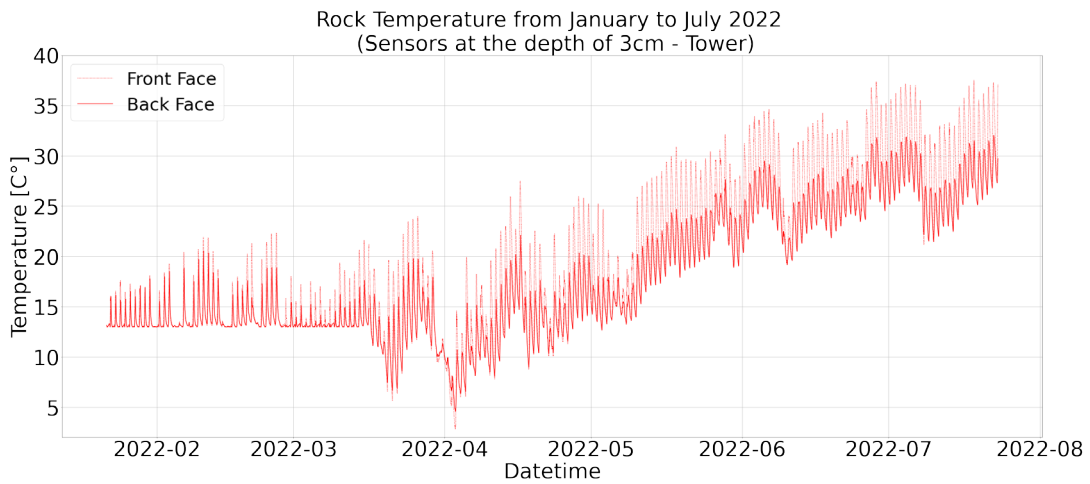


Fig. 14 - Temperature variation measured at 3 cm depth from the surface for both front and back face of the rock tower

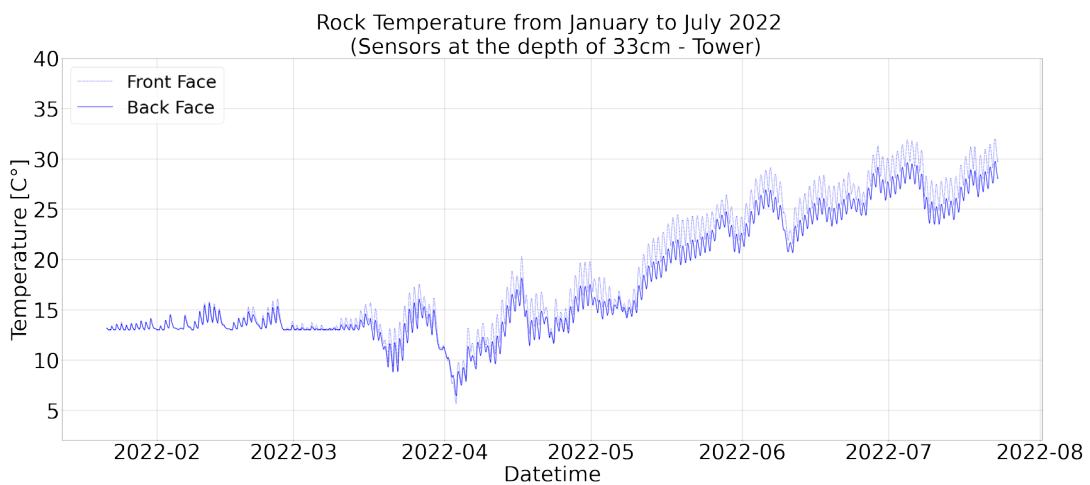


Fig. 15 - Temperature variation measured at 33 cm depth from the surface for both front and back face of the rock tower, in the period from January to July 2022

with solar paths that cause difference in shadowing. Alternatively, if installation issues are excluded, relationships with ventilation can be evoked, since the back face of the rock Tower experiences more frequent wind than the rock Block. Knowing this, the back face of the rock block has the most precise value of the back face temperature of the whole quarry that does not experience wind.

Comparison between IRT and Thermocouples outputs

The use of thermal camera support in assessing the distribution of temperatures at the rock mass surface in a 2D space by converting the emitted radiation into temperatures according to the Stefan Boltzmann law based on the emissivity value of the target object. The FLIR T-840 thermal camera is a high-resolution camera that detects temperature by recognising and capturing different levels of the electromagnetic spectrum in the thermal infrared band. Acquired images were initially calibrated defining the right emissivity value employing a standard reflection method (ASTM) and corrected from parasite radiation and environmental factors that introduce disturbances at increasing distances. Figure 16 shows an example of a picture taken by the thermal camera at Acuto Field Lab in the rock Tower sector.

The thermal camera clearly evidenced the sharp temperature

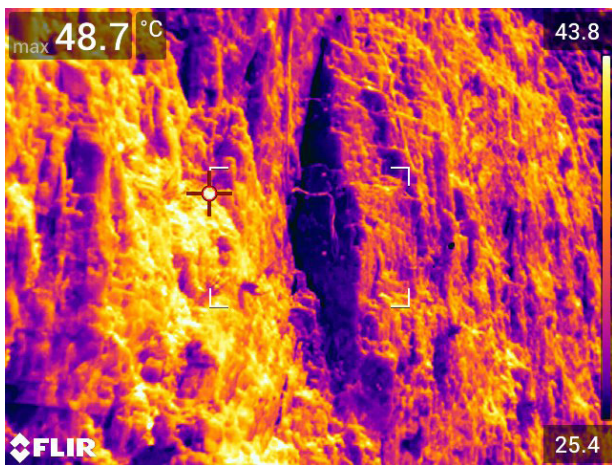


Fig. 16 - Picture taken from the T-840 thermal camera, which frames the rock tower by a East-SouthEast point-of-view

contrast among the two faces, highlighting a cold spot within the opened back fractures. Thermal images were also used to perform a comparison between the values monitored by the sensors installed on the rock face and the ones recorded with the camera. At this aim the acquired pictures of the rock Tower were taken on June 16th, 2022, with a time interval of 1 hour, and were compared with the records from the on-rock sensors. Each photo was taken every hour, starting at 11 a.m. and ending at 6 p.m. By comparing these data with the records at the same date and time from the closest thermocouple installed in the rock, a time temperature variation was plotted (Fig. 17).

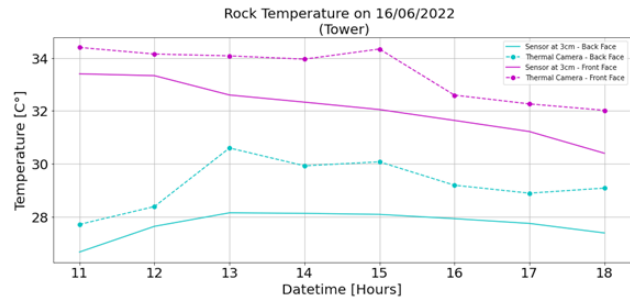


Fig. 17 - Comparison of the temperature values acquired by the thermocouples installed at 3 cm depth on both front and back face of rock tower and then acquires by using the thermal camera

The result leads to two main outcomes: i) temperature values are always higher at the front of the rock Tower than at its back face, which is to be expected as is the part that receives the most sunlight; ii) the camera registers higher temperatures than all the thermocouples, due to the fact that they are not placed exactly on the surface (each at 3 cm depth); at 11:00 the front face experiences its thermal maximum, which is delayed between 1 p.m. and 2 p.m. in the back face. Therefore, we can discuss that the camera registers more accurate surficial temperature data than the thermocouples, accounting for radiative contribution of heat flux. This does not mean that it is the most practical or valuable way of getting information from the rock temperature, given the fact that it is an instrument that needs constant human monitoring and is discontinuous in the acquisition. It may be interesting, for the future of the research, to continue to evaluate the daily behaviour of the temperature with the sensors, and at some strategic days of the year, framing notable elements like fractures and open joints and comparing them in a multitemporal approach to detect evidence of incipient deformation (GUERIN *et alii*, 2019, 2021).

Strain measurements

The specific objective of the strain analysis of the newly instrumented sectors was to get usable data to first compare it to previous results and then search for correlations with the temperature, rain, and wind data. Primarily, a check of the data was performed to find any kind of irregularities in the dataset, also in terms of completeness of the dataset, and to see if something was missing from the first dataset; at this aim a script searching for missing data was codified (Fig. 18)

First let's see what a daily cycle looks like with Fig. 19.

Here we can see first that the strain is at its maximum and then we can see a decrease in strain that we will later correlate with the heating ramp then the temperature rises at its maximum for a bit before going back up along with the cooling ramp. Therefore, in future analysis will be tried to correlate temperature and strain (Fig. 20).

All the data were plotted month by month reporting the daily

EXPLORATIVE DATA ANALYSIS FROM MULTIPARAMETRIC MONITORING AT THE ACUTO FIELD LABORATORY (CENTRAL ITALY) FOR DETECTING PREPARATORY CONDITIONS TO ROCK BLOCK INSTABILITIES

```

CHECK FOR IRREGULARITIES
Entrée [14]: print(1day1,1day2,1day3,1day4,1day5,1day6,1day7)
31 28 30 30 31 30 31

Here we have an issue , March has 31 days and not 30 so that means that some data is missing
we need to find when

Entrée [15]: Bool=True
for i in range (len(donnees)-1):
    Andatetime.strptime(donnees[i]['timestamp'])-1)
    Andatetime.strptime(donnees[i+1]['timestamp'])-1)
    Delta=t-A
    if Delta.seconds !=0:
        Bool=False
        print("Probleme à la donnée (i)")
        print("Ecart de (int(Delta.seconds/60)) minutes entre 2 valeurs consécutives")
if Bool=True:
    print("Aucun problème avec le jeu de donnée")

Probleme à la donnée 38999
Ecart de 61 minutes entre 2 valeurs consécutives
    
```

Fig. 18 - Irregularity check script: it shows the number of data missing between to consecutives data

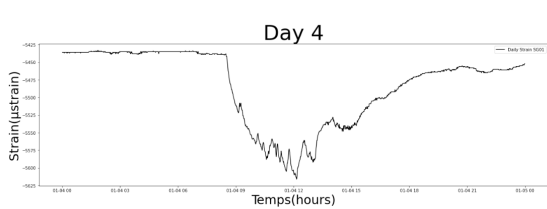


Fig. 19 - Daily Strain cycle in January

maximum, minimum and average values for each strain gauge as reported in Fig. 21. The installed sensors are featured by different initial strain values ranging from -5600 µstrain to -4700

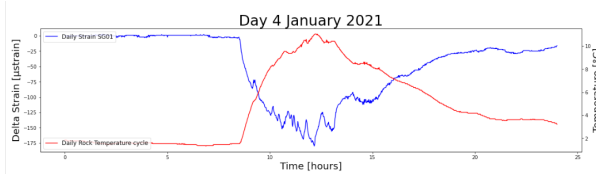


Fig. 20 - Irregularity check script: it shows the number of data missing between to consecutives data

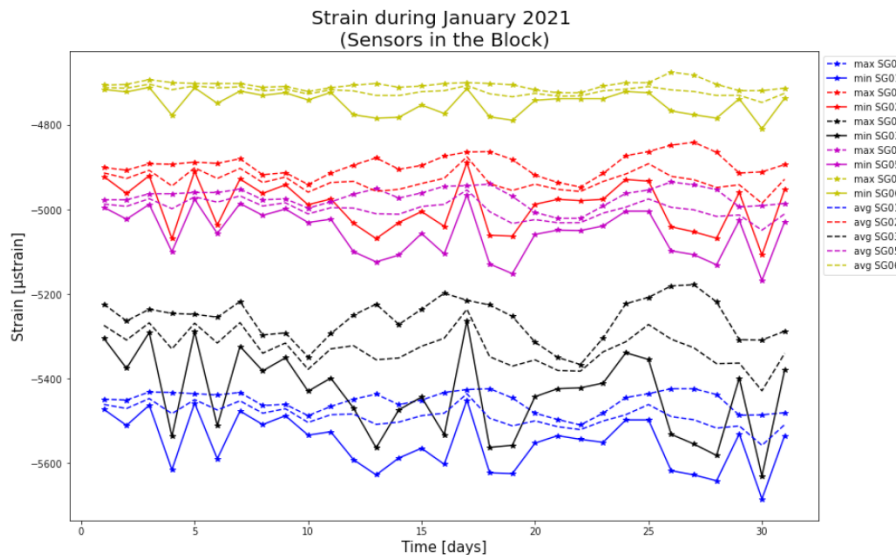


Fig. 21 - Strain gauge recorded data in the rock block, except from the number 4, indicating the maximum and minimum value for each day

µstrain, depending on the initial installation pre-tensioning of the electrical resistance.

Except for the strain gauge number 4, which had some technical problem, all the data shows similar trend with fluctuations that are reciprocally in phase. The rock matrix, where the SG are installed, are exposed to thermal stress due to temperature cycles and direct solar radiation is applied pretty much the same way everywhere in the block. Strain fluctuations appear to be linked with the other datasets (wind/temperature), as evidenced by further analysis that shows an inverse correlation.

The strain data collected in the period were processed analysing it monthly to evaluate seasonal behaviour and highlights potential anomalous trend related to perturbative processes (genetically attributable to rainy or colder months). By the analysis of the zeroed strain series reported in Fig. 22 for the SG06, we can understand that in months characterised by lower temperature, the strain seems to be more stable than in the higher temperature gap months, i.e., July, where the strain varies more as a result of the more intense daily solar radiation.

Also, by plotting rock temperature and strain on the same graph (Fig. 23), it was possible to highlight the already observed anti-correlation between the series: as the temperature increases, both on a diurnal and seasonal scale, the strain decreases and vice versa, thus highlighting cycles of opening-closing of the open joints and expansion-contraction of the rock matrix, also on a dual diurnal and seasonal time scale. This physically confirms the reliability and accuracy of the series in the period.

Correlation between the series is also confirmed by the calculation of correlation factors between temperature (in red) and strain data (blue) (Fig. 24), that results in values equal to -0.99 for Pearson correlation (linear correlation) and -0.99

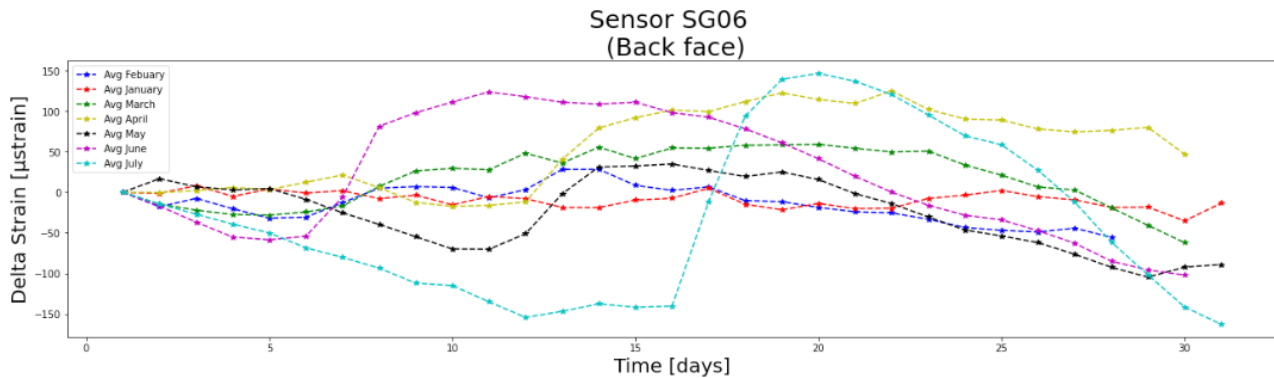


Fig. 22 - Strain gauge recorded data, of sensor number 6 installed on the back face of the rock block, very close to the free surface. Each curve represents a month

for Spearman also (more a nonlinear correlation), with the negative value that remarks the inversely correlated series. When these factors are above 0.7, the correlation between the series/datasets can be stated.

In the graph reported in Fig. 24, the two Pearson and Spearman correlation factors were about -0.1 each, which clearly underlines that, sometimes, due to external factors the

manner the accumulation of strain.

Based and focused on these kinds of outcomes, in the pre-processing we tried to understand the issues in our dataset and locate in time data being not correlated in any days/periods or uncommon behaviours in the daily cycles.

We took for example the month of January 2021 and we categorised 21 days as usual (lowest strain at noon and max

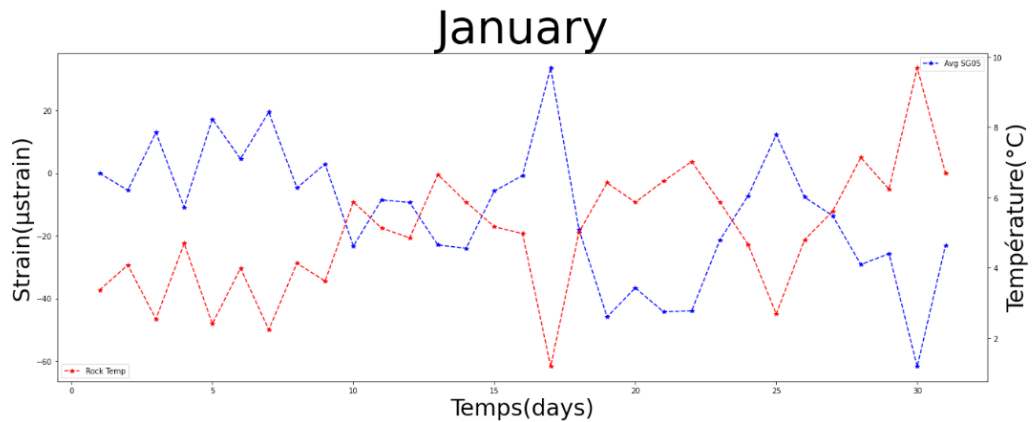


Fig. 23 - Anti-correlation between rock temperature and strain recorded at SG06 on the rock block for the month of January. Strain is in blue while temperature is in red

correlation between strain and temperature can be lacking, even if the trend of the two quantities assumes a comparable trend.

Based and focused on these kinds of outcomes, we tried to calculate the residual strain over a year, by stacking it from the beginning and by seeing how much residual strain was accumulated in the rock block (Fig. 25). Unfortunately, the adopted method was a little too basic for such a specific natural environment and we did not take enough parameters into account which resulted in a flawed result; anyway, the data was still a bit interesting because we could see on a linear

during the night) and 10 days as strange behaviours, which are January 2021, 1st, 2nd, 3rd, 5th, 9th, 11th, 17th, 23rd, 24th and 31st. For those days the strain just oscillated during the whole day without any pattern. Seeing this we tried to explain why sometimes there was, especially in January days, aperiodic behaviours. To understand this was realised an algorithm to detect if there were peculiar weather conditions like fog, or rock freezing (Fig. 26). Adopting as input parameters a rock temperature lower than 0 °C, rainfalls occurred within 10 hours before the time selected and finally a humidity rate of 100%.

So, the 26th of January is considered a day when a freezing

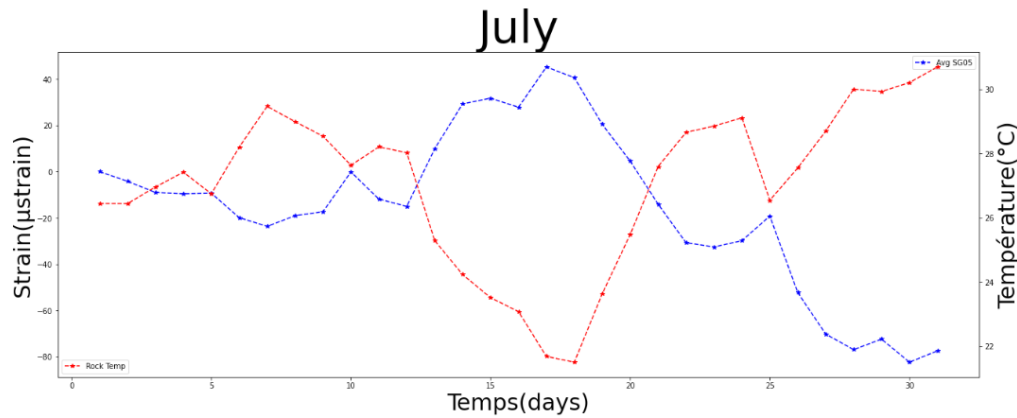


Fig. 24 - Anti-correlation between rock temperature and strain recorded at SG06 on the rock block for the month of July. Strain is in blue while temperature is in red

```
Entrée [59]: ResJan2imp.zeros(Ndays)
j=0
for i in range (Ndays):
    if AvgDay[i]!=0:
        ResJan[i]=Sub(AvgDay[i]-AvgDay[21])
        if Check[i]==10:
            print('Residual strain over a year in January in day (i+1) is (ResJan[i]) Précision Faible (Check[i] valeurs)')
        if Check[i]==10 and Check[i+3]==8:
            print('Residual strain over a year in January in day (i+1) is (ResJan[i]) Précision Moyenne (Check[i] valeurs)')
        if Check[i]==10:
            print('Residual strain over a year in January in day (i+1) is (ResJan[i]) Précision Grande (Check[i] valeurs)')
        j=j+1
Residual strain over a year in January in day 1 is 120.0 Précision Grande 44 valeurs
Residual strain over a year in January in day 2 is 67.0 Précision Grande 34 valeurs
Residual strain over a year in January in day 3 is 75.0 Précision Grande 32 valeurs
Residual strain over a year in January in day 4 is 104.0 Précision Grande 33 valeurs
Residual strain over a year in January in day 5 is 71.0 Précision Grande 30 valeurs
Residual strain over a year in January in day 6 is 66.0 Précision Moyenne 29 valeurs
Residual strain over a year in January in day 7 is 42.0 Précision Faible 6 valeurs
Residual strain over a year in January in day 8 is 20.0 Précision Grande 34 valeurs
Residual strain over a year in January in day 9 is 43.0 Précision Faible 6 valeurs
Residual strain over a year in January in day 11 is 1.0 Précision Moyenne 25 valeurs
Residual strain over a year in January in day 12 is 22.0 Précision Moyenne 29 valeurs
Residual strain over a year in January in day 13 is 35.0 Précision Grande 34 valeurs
Residual strain over a year in January in day 14 is 63.0 Précision Grande 35 valeurs
Residual strain over a year in January in day 15 is 75.0 Précision Grande 34 valeurs
Residual strain over a year in January in day 16 is 104.0 Précision Faible 4 valeurs
Residual strain over a year in January in day 17 is 105.0 Précision Faible 1 valeurs
Residual strain over a year in January in day 22 is 19.0 Précision Grande 32 valeurs
Residual strain over a year in January in day 23 is 105.0 Précision Faible 1 valeurs
Residual strain over a year in January in day 24 is 9.0 Précision Grande 34 valeurs
Residual strain over a year in January in day 25 is 36.0 Précision Grande 32 valeurs
Residual strain over a year in January in day 26 is 65.0 Précision Grande 33 valeurs
Residual strain over a year in January in day 27 is 67.0 Précision Grande 32 valeurs
Residual strain over a year in January in day 28 is 44.0 Précision Grande 33 valeurs
Residual strain over a year in January in day 29 is 11.0 Précision Grande 33 valeurs
Residual strain over a year in January in day 30 is 4.0 Précision Moyenne 25 valeurs
Residual strain over a year in January in day 31 is 1.0 Précision Faible 7 valeurs
```

Fig. 25 - Script for the residual strain calculation: example of calculation

```
Check=[]
minV=[]
maxV=[]
minV.append(10000000000000000000)
maxV.append(0)
k=0
for i in range (Ndatatot-1):
    Test=False
    if Test[i]==0:
        for j in range (1,i+60):
            if (Stat[j]==0) or Test[j]==100:
                Test=True
            if Test==False:
                Check.append(False)
            else:
                Check.append(True)
        else:
            Check.append(False)
    for j in range (len(Check)):
        if Check[j]==True:
            if minV[k]>Tempdate[j].hour*60-Tempdate[j].minute:
                minV[k]=Tempdate[j].hour*60-Tempdate[j].minute
            if maxV[k]<Tempdate[j].hour*60-Tempdate[j].minute:
                maxV[k]=Tempdate[j].hour*60-Tempdate[j].minute
        if Check[j]==True and Check[j+1]==False:
            print('Potential Freezing on (Tempdate[j].day) of (Mois[Tempdate[j].month-1]) from (minV[k]/60)h:(maxV[k]/60) to (k+1)')
            minV.append(10000000000000000000)
            maxV.append(0)
            k=k+1
Potential freezing on 26 of January from 6h:31 to 7h:4
Potential freezing on 14 of February from 5h:55 to 7h:56
```

Fig. 26 - Script for the freezing detection and weather singularity days

event happens, as all the input conditions are met. Therefore, the freezing impact on our dataset happened a bit after starting on the 21st of January and going on during February, highlighting the period during the year in which the freezing conditions are most anticipated.

Finally, the graph in Fig. 27 shows that temperature and strain are generally correlated along our dataset spanning from

the Winter 2021 to Summer 2022. Given the Acuto Field Lab renovation and the installation of new monitoring devices, the period from November 2021 to March 2022 had less data.

The same analysis was also carried out for the rock tower sector data (Fig. 28), the last to be instrumented in January 2022. Data pre-processing allows to evaluate data completeness and issues in the data logging. Some issues were found and consequently fixed: i) a temperature minimum cutoff (Tmin locked at a 13°C) ii) a rising drift in the SG01 (tower sector) potentially related either to installation error or placement in a more detached zone or glueing and sticking of electrical resistance on the rock surface.

Finally, as for the rock Block, Fig. 29 reports the final graph for the rock tower sector and the same as before on the extended period, temperature, and strain series correlation.

Vibrations analysis

The primary objective of the vibrations preliminary analysis was to evaluate the capability of recording different kinds of vibrations over the monitored sectors, by checking the collected time histories. A following research objective will be the investigation of the influence of the earthquakes and/or microseismicity on the rock wall deformation, and therefore, on their effects to fractures growth leading to instability. Specific routines were written in MATLAB to rearrange the data recorded by the 13 geophones and create one-hour long SAC files, from which mean and trend were removed. In the following, a first check of the time histories was done to verify the presence of earthquakes within them. By referring to the website of the “Istituto Nazionale di Geofisica e Vulcanologia” (<http://terremoti.ingv.it/>), a list of the occurred earthquakes with a searching radius of 100 km around the Acuto municipality was obtained.

Figure 30 reports an exemplary time history recorded by a geophone located at the rock Tower sector on 27th of February 2022 from 7am to 8am: this time interval is concomitant with the M_w 3.0 earthquake which occurred on 27th of February 2022

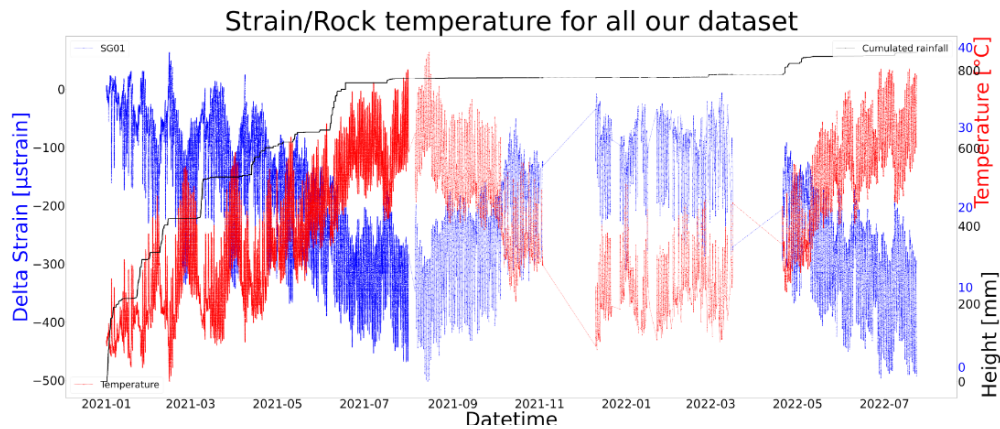


Fig. 27 - Synoptic view of the rock block monitoring data during the entire period. Temperature is reported in red, strain in blue, and cumulative rain in black

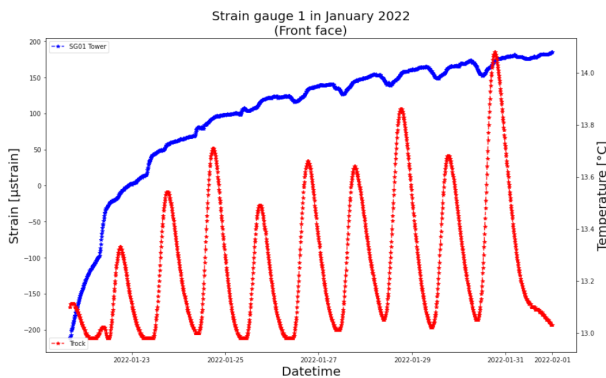


Fig. 28 - Temperature (red) and strain (blue) series recorded in the rock tower sector. The fixed minimum temperature cutoff at 13 °C and the anomalous trend of the values are visible

signal of an earthquake. In general, it was observed very weak or even zero response in conjunction with earthquakes. This is mainly because no relevant earthquakes (in terms of magnitude) occurred in the analysed period, moreover they were located quite far from the Acuto municipality, therefore attenuation might have prevented their recording by the geophones.

Figure 31 shows peaks for the horizontal components that could be related to vibrations inside the rock wall: the absence of the same peak on the vertical component let us exclude an electrical spike such signal shapes, known as microseismic (MS) events or can be related to a local fracturation phenomena occurred because of thermal and mechanical stresses. The link between these kinds of signals and the effects produced by thermal and mechanical stresses needs to be further investigated, therefore an inventory of microseismic signals collected on

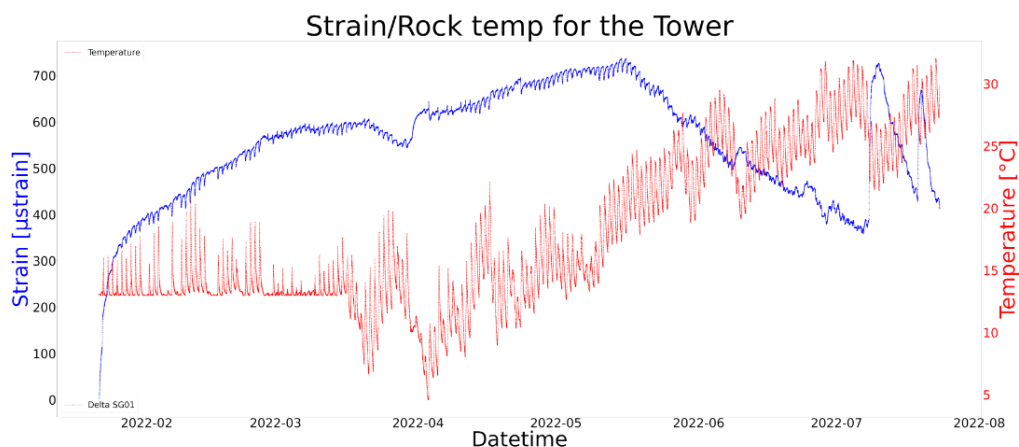


Fig. 29 - Temperature, strain a rainfall time series recorded in the rock tower sector. The error in the temperature time series and its overcoming is reported

at 07:31:58 at Amatrice, about 90 km far from Acuto. Despite there are no vibrations recorded on the vertical component, some occur on the horizontal ones, but are not related to the typical

the rock would be fundamental to approach this research topic. Moreover, the collected waveforms can be both useful for classification purposes (based on signal shape and energy

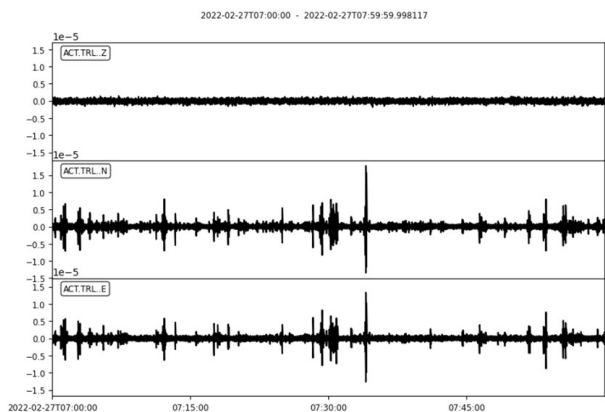


Fig. 30 - Graph representing the time histories (top: up-down; middle: North-South; bottom: East-West) recorded by a geophone located at the rock Tower sector on 2022-02-27 from 07:00:00 to 08:00:00

content) and for testing novel analysis approaches (D'ANGIÒ *et alii*, 2021a). Lastly, another future perspective, consist of approaching MS events source location and parameterization, by taking advantage of the wide geophones network deployed at the different sectors. Of particular interest will be the analysis of the data related to the rock Block and Tower zones, for which there will be a large availability of vibrational data, allowing both the comparison of signals characteristics between front and back sides and between lower and upper portion of the rock Tower.

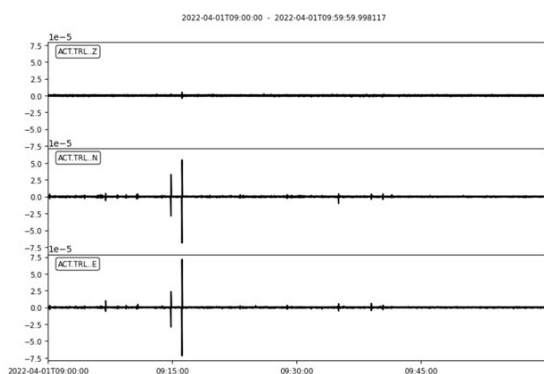


Fig. 31 - Graph reporting an example of a microseismic event recorded on a geophone installed on the rock Tower sector on 2022-04-01 from 09:00:00 to 10:00:00

CONCLUSION AND PERSPECTIVES

The conducted study, started after the instrumental integration of the Acuto Field Lab (Frosinone, Italy), allows to evaluate data consistency and accuracy of the newly installed sensor, fixing polynomial conversion and transmission bugs from the devices to the acquisition units locate in the shelter at the top of the quarry cliff.

From our study, we first confirm that the most relevant anti-

correlation was between the stress and rock temperature data, both at the tower and block level. The quarry is exposed to solar radiation for most of the day, resulting in large temperature changes that cause a great deal of stress due to the expansion and contraction of the rock. This stress, which slowly builds up over the days, can lead to instability of the quarry wall with fracture formation or progression and extension of fracture length at their tips. The rock mass is also highly fractured (5 different penetrating joint sets) and is therefore prone to collapse under the continuous action of preparatory forcings (climate-related) or triggers (intense rainfall, earthquakes, human vibrations). One of these factors, from a deterministic analysis on strain time-series, wind, appear not very influential. Despite this, quantitative evaluation by vibration modal analysis on natural frequency can be approached by multitemporal, and spatially differential spectral ratios. Rainfall is one of the most intuitive triggering factors. It percolates inside the joints and can increase their width or also freeze during the winter months causing instability due to cryoclastic phenomena. This mechanism is one of the most effective in the site, as recently observed from MS monitoring after the 2018 Buran winter storm (D'ANGIÒ *et alii*, 2021b). MS events have proved to be diagnostic of the environmental conditions, which controls the stress state regime (critical/subcritical; GRECHI, 2022). As for the registered vibrational signals, no major earthquakes were felt in the site during the analysed period. Nevertheless, microseismic events were observed: their characterisation in terms of magnitude and location of the source will be evaluated in the future. In addition, the temporal progression of the major MS events, and their relationship with the continuous acoustic emission released by the rock matrix will be computed, considering mutual direct or cross correlation with the environmental stressors in view of understanding precursors of instabilities at different scales.

ACKNOWLEDGEMENTS

This study is part of the internship of 4 Master of Earth Science Engineering students at Polytech Sorbonne supervised by the Department of Earth Sciences of the Sapienza University of Rome. The authors would like to thank their tutor Salvatore Martino, professor at the University, for having accompanied us and integrated us into his team in the CERI-Research Centre for Geological Risk laboratory.

The authors would like to thank Sapienza University of Rome for hosting them for 9 weeks and Sorbonne University for allowing them to complete this internship. The authors also wish to thank the municipality of Acuto for its support of the experimental activities in the quarry.

The research is framed in the projects "Dipartimenti di Eccellenza 2018-2022" founded by the Italian Ministry of Universities and Research (MUR), attributed to the Department of Earth Sciences of the Sapienza University of Rome, and "Approcci di Artificial Neural Network per analisi di dati

da sistemi di monitoraggio multi-parametrico applicati alla mitigazione del rischio da frana: comprensione intelligente delle relazioni causa-effetto tra forzanti e deformazioni indotte e previsione delle condizioni di rottura” (Year 2021 - P.I. Matteo Fiorucci, Ph.D.).

AUTHOR CONTRIBUTIONS

A.C. Le Gallais processed and analysed the meteorological data under the supervision of D. D'Angiò, G. Grechi, and R. Iannucci. J. Rosa Fernandes processed and analysed the

temperature and IR thermography data under the supervision of G.M. Marmoni, G. Grechi, M. Fiorucci, and G. Amato. H. Sampieri processed and analysed the stress data under the supervision of G.M. Marmoni, M. Fiorucci, and G. Amato. J.P. Hu processed and analysed the microseismic data under the supervision of D'Angiò G. Grechi, and R. Iannucci. Together they planned the data processing and S. Martino coordinated the research activity and planned the experimental phases. All authors discussed the proposed approach, provided an interpretation of the results, and wrote the paper.

REFERENCES

- BAKUN-MAZOR D., HATZOR Y.H., GLASER S.D. & SANTAMARINA J.C. (2013) - *Thermally vs. seismically induced block displacements in Masada rock slopes*. Int. J. Rock Mech. Min., **61**: 196-211.
- BOTTELIN P., JONGMANS D., BAILLET L., LEBOURG T., HANTZ D., LÉVY C., LE ROUX O., CADET H., LORIER L., ROUILLER J-D., TURPIN J. & DARRAS L. (2013) - *Spectral analysis of prone-to-fall rock compartments using ambient vibrations*. J. Environ. Eng. Geophys., **18**(4): 205-217.
- CARSLAW H.S. & JAEGER J.C. (1959, Eds.) - *Conduction of Heat in Solids*. 2nd ed; Clarendon Press, Oxford, UK.
- COLLINS B.D., STOCK G.M. & EPPES M.C. (2019) - *Relaxation response of critically stressed macroscale surficial rock sheets*. Rock Mech. Rock Eng., **52**(12): 5013-5023.
- COLLINS B.D. STOCK G.M., EPPES M.C., LEWIS S W., CORBET, S C. & SMITH J.B. (2018) - *Thermal influences on spontaneous rock dome exfoliation*. Nat. Commun., **9**(1): 1-12.
- D'ANGIÒ D., LENTI L. & MARTINO S. (2021a) - *Microseismic monitoring to assess rock mass damaging through a novel damping ratio-based approach*. Int. J. Rock Mech. Min., **146**: 104883.
- D'ANGIÒ D., FANTINI A., FIORUCCI M., IANNUCCI R., LENTI L., MARMONI G.M. & MARTINO S. (2021b) - *Environmental forcings and micro-seismic monitoring in a rock wall prone to fall during the 2018 Buran winter storm*. Nat. Hazards, **106**(3): 2599-2617.
- FINNEGAN R., MOORE J.R. & GEIMER P.R. (2022) - *Contribution of anthropogenic vibration sources to crack growth in natural rock arches*. Front. Earth Sci., **10**: 1035652.
- FANTINI A., FIORUCCI M., MARTINO S. & SARANDREA P. (2017) - *3D Remote survey of a rock wall hosting a multi-sensor monitoring system in a test-site (Acuto, Italy)*. Rend. Online Soc. Geol. Ital., **42**: 30-33.
- FIORUCCI M., MARMONI G.M., MARTINO S. & MAZZANTI P. (2018) - *Thermal response of jointed rock masses inferred from infrared thermographic surveying (Acuto test-site, Italy)*. Sensors, **18**(7): 2221.
- FIORUCCI M., MARTINO S., BOZZANO F. & PRESTININZI A. (2020) - *Comparison of approaches for data analysis of multi-parametric monitoring systems: insights from the Acuto test-site (Central Italy)*. Appl. Sci., **10**(21): 7658.
- GASC-BARBIER, M. & MERRIEN-SOUKATCHOFF, V. (2019) - *Effect of Natural Thermal Cycles on Rock Slopes Stability-Study of 2 French Sites*. In: FONTOURA S.A.B., ROCCA R. & MENDOZA J. (2019, eds.) - *Rock Mechanics for Natural Resources and Infrastructure Development*, 3514-3521, CRC Press, London.
- GEIMER P.R., FINNEGAN R. & MOORE J.R. (2022) - *Meteorological controls on reversible resonance changes in natural rock arches*. J. Geophys. Res. Earth Surf., **127**(10): e2022JF006734.
- GISCHIG V.S., MOORE J.R., EVANS K.F., AMANN F. & LOEW S. (2011a) - *Thermomechanical forcing of deep rock slope deformation: 1. Conceptual study of a simplified slope*. J. Geophys. Res. Earth Surf., **116**(F4): F04010.
- GISCHIG V.S., MOORE J.R., EVANS K.F., AMAN, F. & LOEW S. (2011b) - *Thermomechanical forcing of deep rock slope deformation: 2. The Randa rock slope instability*. J. Geophys. Res. Earth Surf., **116**(F4): F04011.
- GRECHI G. (2022) - *Nonlinear strain effects induced by thermal forcing on jointed rock masses*. Ph.D. Thesis. Sapienza University of Rome, Department of Earth Sciences.
- GRECHI G., FIORUCCI M., MARMONI G.M. & MARTINO S. (2021) - *3D thermal monitoring of jointed rock masses through infrared thermography and photogrammetry*. Remote Sens., **13**(5): 957.
- GUERIN A., JABOYEDOFF M., COLLINS B.D., DERRON M.H., STOCK G.M., MATASCI B., BOESIGER M., LEFEUVRE C. & PODLADCHIKOV Y.Y. (2019) - *Detection of rock bridges by infrared thermal imaging and modeling*. Sci. Rep., **9**(1): 1-19.
- GUERIN, A. JABOYEDOFF M., COLLINS B.D., STOCK G.M., DERRON M.H., ABELLÁN A. & MATASCI B. (2021) - *Remote thermal detection of exfoliation sheet deformation*. Landslides, **18**(3): 865-879.

EXPLORATIVE DATA ANALYSIS FROM MULTIPARAMETRIC MONITORING AT THE ACUTO FIELD LABORATORY (CENTRAL ITALY) FOR DETECTING PREPARATORY CONDITIONS TO ROCK BLOCK INSTABILITIES

- GUILLEMOT A., BAILLET L., LAROSE E. & BOTTELIN P. (2022) - *Changes in resonance frequency of rock columns due to thermoelastic effects on a daily scale: observations, modelling and insights to improve monitoring systems*. *Geophys. J. Int.*, **231**(2): 894-906.
- GUNZBURGER Y., MERRIEN-SOUKATCOFF V. & GUGLIELMI, Y. (2005) - *Influence of daily surface temperature fluctuations on rock slope stability: case study of the Rochers de Valabres slope (France)*. *Int. J. Rock Mech. Min.*, **42**(3): 331-349.
- HUNGR O., LEROUÉIL S. & PICARELLI L. (2014) - *The Varnes classification of landslide types, an update*. *Landslides*, **11**(2): 167-194.
- MARMONI G.M., FIORUCCI M., GRECHI G. & MARTINO S. (2020) - *Modelling of thermo-mechanical effects in a rock quarry wall induced by near-surface temperature fluctuations*. *Int. J. Rock Mech. Min.*, **134**: 104440.
- TABOADA A., GINOUEZ H., RENOUF M. & AZEMARD P. (2017) - *Landsliding generated by thermomechanical interactions between rock columns and wedging blocks: Study case from the Larzac Plateau (Southern France)*. In: *EPJ Web of Conferences*, **140**:14012, EDP Science.

Received November 2022 - Accepted December 2022